

PROCEEDINGS OF SPIE

[SPIDigitalLibrary.org/conference-proceedings-of-spie](https://spiedigitallibrary.org/conference-proceedings-of-spie)

Transient differential pressure-induced loss variation in as-drawn hollow core optical fibres

Shuichiro Rikimi, Thomas Kelly, Peter Horak, Yong Chen, Ian Davidson, et al.

Shuichiro Rikimi, Thomas W. Kelly, Peter Horak, Yong Chen, Ian A. Davidson, Simon Bawn, Thomas D. Bradley, Austin A. Taranta, Francesco Poletti, David J. Richardson, Natalie V. Wheeler, "Transient differential pressure-induced loss variation in as-drawn hollow core optical fibres," Proc. SPIE 12140, Micro-Structured and Specialty Optical Fibres VII, 1214002 (19 May 2022); doi: 10.1117/12.2621301

SPIE.

Event: SPIE Photonics Europe, 2022, Strasbourg, France

Transient differential pressure-induced loss variation in as-drawn hollow core optical fibres

Shuichiro Rikimi ^{*a}, Thomas W. Kelly ^a, Peter Horak ^a, Ian A. Davidson ^a, Yong Chen ^{a,b}, Simon Bawn ^b, Thomas D. Bradley ^a, Austin A. Taranta ^a, Francesco Poletti ^a, David J. Richardson ^{a,b} and Natalie V. Wheeler ^a

^aOptoelectronics Research Centre, University of Southampton, Southampton SO17 1BJ, U.K.;

^bLumenisity Ltd, Unit 7, The Quadrangle, Premier Way, Romsey, U.K.

ABSTRACT

We demonstrate transient changes in the optical properties, specifically the loss, of antiresonant hollow core fibres (HCFs) due to a combination of the sub-atmospheric gas pressure inside the fibre holes post-fabrication and the subsequent gas-induced differential refractive index (GDRI) between the core and cladding elements of the fibre; this is temporarily created while the gas pressures inside the core and cladding elements are evolving after the HCF ends are opened up to surrounding atmospheric pressure. Here we show experimental evidence of this effect in two different HCF designs; for both fibres, the transmitted power initially increases, reaches a maximum, and then reduces to its initial level. We show via gas flow simulations that the timeline of this behaviour is consistent with the gas flow rates into the core and cladding elements of the tubular HCF studied and the subsequent transient differential gas pressure. The experimental results also show (in line with GDRI expectations) that this transmission (loss) change is higher at shorter wavelengths. Our results imply that this transient change in the fibre's optical properties must be considered for accurate fibre characterisation; this is particularly true for long fibre lengths where the equalisation of the fibre's internal gas pressure with atmospheric pressure could take many weeks.

Keywords: Hollow core fibres, loss, characterisation

1. INTRODUCTION

Hollow core optical fibres (HCFs) are a specialty fibre, where light is guided in a gas-filled core, surrounded by a microstructured cladding. The advantages of light transmission in gas (usually air) are such that HCFs are being applied in diverse application areas including telecommunications, high power delivery and gas sensing [1-3]. For these applications, accurate and reliable characterisation of the optical properties of these fibres is essential; for example, over- or under-estimation of the fibre loss will cause problems in system design. Furthermore, it is critical that the HCF's optical properties remain consistent when the fibre is deployed as if this is not the case, this will impact the overall system performance.

Recent work has shown that the optical properties of a HCF can be significantly changed by introducing a gas-induced differential refractive index (GDRI) between the core and cladding elements of the fibre [4]. Practically, this can be implemented by introducing a higher or lower gas pressure in the core as opposed to the cladding. Parallel work has also shown that the gas pressure inside a HCF immediately after fabrication is substantially below atmospheric. This means that once a HCF is exposed to atmospheric pressure post-fabrication, the resulting pressure difference drives gas flow into the holes of the HCF [5]. The fill-time for the core and cladding holes of the HCF will be different due to the different hole sizes [6] and therefore, while the pressure inside the HCF holes is increasing to atmospheric, the larger diameter core will fill faster than the cladding. This should create a transient differential pressure (and hence GDRI) between the core and cladding elements which could lead to transient changes in the optical properties of the fibre.

Here we show, for the first time, evidence of this effect and the impact on the fibre's transmission loss post-fabrication, while the pressure is equalising. Transmission spectra of a Nested Antiresonant Nodeless Fibre (NANF) and a tubular HCF were continuously recorded after opening the sealed fibre end(s) to atmosphere; these ends were previously sealed immediately after fabrication. The results show that the transmitted power initially increased and then over time returned to a level similar to the initial transmission. The timescales of these changes are consistent with gas flow predictions based on the fibre geometries and lengths. The results also show that these temporary changes in transmission are more significant at shorter wavelengths. These results are in line with expectations due to GDRI; the transient higher pressure in the core, raises the effective index of the core guided modes relative to the cladding modes, reducing confinement and bend loss [4]. Once the cladding pressure also equalises to atmospheric, the loss then increases again. Comparison with

gas flow dynamics modelling supports these results. Knowledge and understanding of the magnitude and time dynamics of this transient change in HCF's optical properties are essential for accurate characterisation post-fabrication, to avoid inaccurate loss measurements and to ensure consistent optical performance of the fibre during deployment. This is particularly important for long fibre lengths, where, due to the scale of the fibre structure, the time for pressure equalisation could extend to weeks.

2. EXPERIMENTAL RESULTS AND ANALYSIS

2.1 Fibre characteristics

In this work, two types of HC-ARFs were studied: a NANF and a tubular HCF. Scanning electron microscope (SEM) images of these HCFs are shown in Fig. 1(a) and Fig. 2(a) respectively. The NANF used in section 2.2 has a $32.4\ \mu\text{m}$ diameter core which is defined by five pairs of $31.4 \pm 0.6\ \mu\text{m}$ diameter outer tubes and $13.2 \pm 0.3\ \mu\text{m}$ diameter inner tubes. The tubular HCF used in section 2.3 consists of seven $10.1 \pm 0.2\ \mu\text{m}$ diameter outer tubes which define a $18.6\ \mu\text{m}$ diameter core.

In this paper, we use the term 'as-drawn fibre' to describe fibres for which the two ends of each fibre are sealed immediately after fabrication in order to preserve the initial internal sub-atmospheric pressure [5] until any characterisation experiments are carried out; both the NANF and tubular HCFs used in this work were prepared in this way. In the following experimental sections, the impact of the initial as-drawn pressure equalising with atmospheric pressure was measured by monitoring changes in transmitted power through the as-drawn HCFs when their ends were opened up to standard atmospheric pressure.

2.2 Transmission spectra measurement of an as-drawn NANF

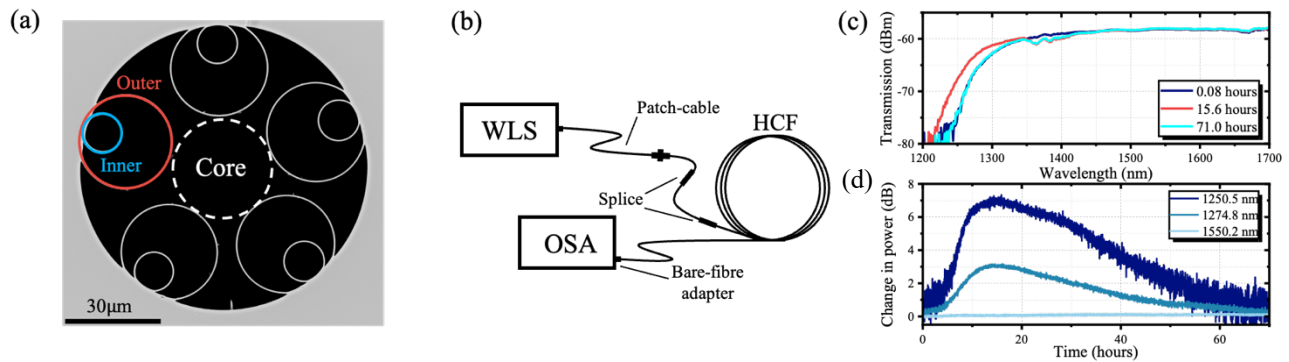


Fig. 1. (a) A SEM image of the NANF. (b) The experimental setup of the transmission measurement using the NANF. The components shown are a white light source (WLS), a single mode patch cable, a hollow core fibre (HCF), and an optical spectrum analyser (OSA) and a bare fibre adapter. (c) The transmission spectrum through the 100 m NANF assembly at 0.08 hours (dark blue), 15.6 hours (red) and 71 hours (light blue) after cleaving off the sealed HCF end. (d) The change in transmitted power for three selected wavelengths.

For the first investigation, the transmission spectrum through 100 m of as-drawn NANF (Fig. 1(a)) was measured after the ends were cleaved to open up the holes within the fibre to atmospheric pressure. Prior to the experiment, one optical input end of the NANF was hermetically fusion spliced to solid fibre (a large mode area fibre and a FC/APC pigtail). The time for which this end of the HCF was exposed to the atmosphere during this splicing process was 1.5 minutes and during this time gas from the atmosphere would have been able to flow into the fibre's microstructure; the other (output) end of the HCF remained sealed during the splicing process. The schematic of the experimental setup is shown in Fig. 1(b). The spliced end was mechanically connected to a white light source (WLS), and this ensured that the optical launching condition was consistent during the subsequent experiment. The seal on the output end of the HCF end was cleaved off just before starting the measurement and connected to an optical spectrum analyser (OSA) using a bare fibre adapter which allowed surrounding atmospheric gas to flow into the HCF. The transmission spectrum through the NANF assembly was continuously recorded over the following 71 hours.

Fig. 1(c) shows the transmission spectra from the NANF assembly 0.08 hours, 15.6 hours and 71 hours after opening the sealed HCF end. The spectra noticeably changed during the experiment; the short wavelength edge of the transmission window shifted by a maximum of $\sim 35\ \text{nm}$ to shorter wavelengths. In contrast, changes were not observed in the longer wavelength range ($\sim 1450\ \text{nm}$ and beyond). Some of the changes in the transmission between 1340 and 1450 nm can be attributed to water vapour absorption within the hollow core, a result of the ingress of the air into the hollow core. However,

this does not explain the changes at wavelengths outside of the water vapour absorption range. The transmitted power for three selected wavelengths is presented with respect to time in Fig. 1(d), highlighting the time dependent behaviour of the transmission changes recorded at the short wavelength edge; the transmitted power increases up to a time of ~ 15.6 hours and then gradually reduces to the initial level. Also, the wavelength-dependent feature is clearly illustrated in Fig. 1(d); the change in the transmitted power was significant at the shorter wavelength compared to the longer wavelength.

Since the HCF used here was kept in an as-drawn condition prior to the experiment and therefore the voids within the fibre contained gas at sub-atmospheric pressure, this result suggests that the atmospheric flow into the HCF due to the pressure difference between inside the fibre and the atmosphere could be related to the observed transmitted power dynamics. In particular, the wavelength dependence observed is consistent with the GDRI effect [4], implying that the low post-fabrication pressure could potentially induce the GDRI effect. When the as-drawn HCF is opened up to atmospheric gas pressure, the gas filling time for the hollow core and cladding air holes differs as $t_{fill} \propto (L/2r)^2$ where L is the fibre length and r is the hole radius [6], changing the fibre attenuation by the GDRI effect. However, to further investigate the observed changes in transmission we repeat this experiment with a tubular HCF and compare with a gas flow model.

2.3 As-drawn pressure induced loss transition in a tubular HCF

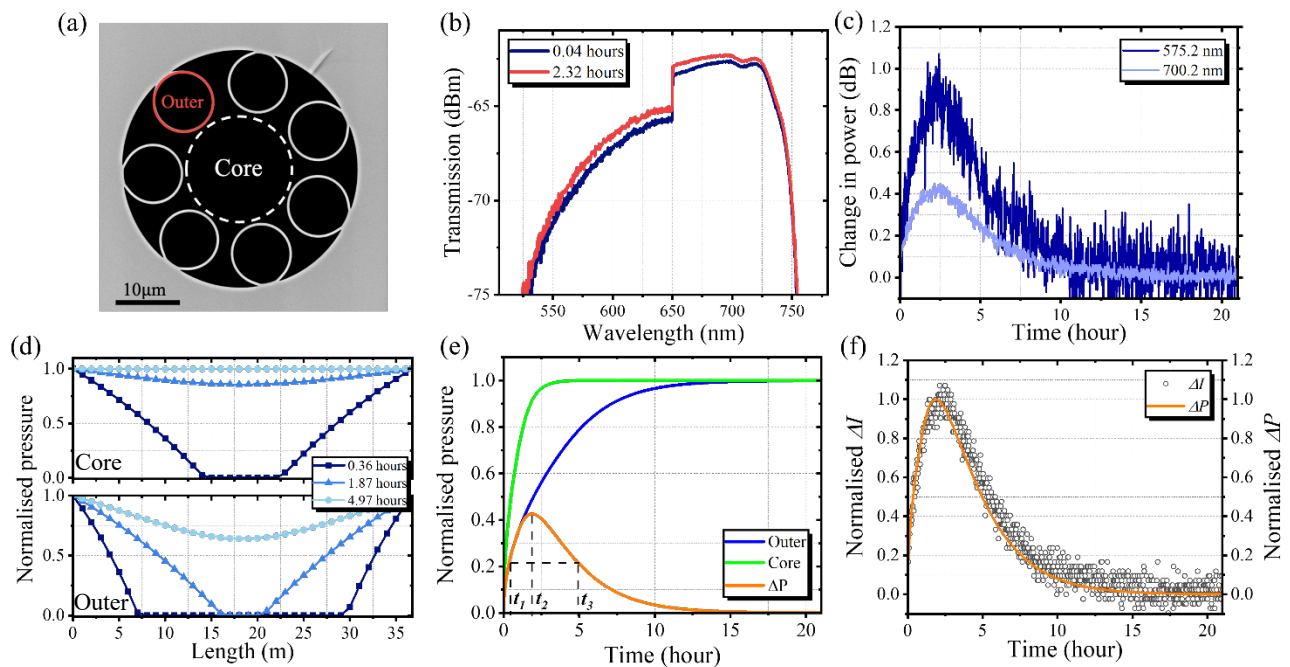


Fig. 2. (a) A SEM image of the tubular HCF. (b) The transmission spectrum through the 26.75 m tubular HCF at 0.04 hours (dark blue) and 2.32 hours (red) after cleaving off the sealed HCF ends (Note: discontinuity at ~ 650 nm is due to a change in grating within the OSA used for detection). (c) The change in transmitted power for two selected wavelengths. (d) Numerical results showing the spatial variation of air pressure in the core ($2r_{core} = 18.6 \mu\text{m}$) and the outer tube ($2r_{outer} = 9.29 \mu\text{m}$) using Eq. (1) for 0.36 hours, 1.87 hours and 4.97 hours. (e) Numerical results of the average pressure inside the core (green) and the outer tube (dark blue) using Eq. (1) with $2r_{core} = 18.6 \mu\text{m}$ for the core and $2r_{outer} = 9.29 \mu\text{m}$ for the outer. The orange solid line is the calculated differential pressure (ΔP) between the core and the outer tube. t_1 , t_2 and t_3 correspond to 0.36 hours, 1.87 hours and 4.97 hours, respectively, which are selected in Fig. 2(d). (f) Comparison between the calculated normalised ΔP shown in Fig. 2(e) and the measured normalised transmitted power at 700.2 nm (ΔI , open circle) shown in Fig. 2(c).

The result in section 2.2 indicates that the atmospheric flow into the HCF could drive the transient changes in the loss of the as-drawn HCF; the increase/decrease in the transmitted power could result from the changes in loss due to the differential pressure between the hollow core and the cladding tubes. To understand the pressure effect further, evolution of transmitted power was measured using 36.75 m of the as-drawn tubular HCF (Fig. 2(a)); this simpler structure, without the nested inner element, is advantageous for comparison with a gas flow model. The experimental setup was the same as in Fig. 1(b), however for this test neither ends of the HCF were spliced with a solid fibre, and therefore the HCF ends were connected directly to the WLS and the OSA (ensuring consistent optical launch) using bare fibre adapters and the ingress of the atmosphere occurred from both ends. The data acquisition started 2.4 minutes after opening the fibre ends and then the transmission spectrum was continuously recorded over the following 21 hours. The transmission spectra for two selected times and the evolution of the transmitted power at two different wavelengths are shown in Fig. 2(b) and

(c). The features of the increase/decrease in the transmitted power with the wavelength dependence observed are very similar to the NANF measurement, albeit over different timescales; the transmitted power reached a maximum at ~2.3 hours and then gradually decreased for the following ~13 hours. The transmission change was also again higher at shorter wavelengths.

To consider whether the timescales of these observed transmission changes are consistent with expected gas pressure changes inside the HCF's microstructure, the gas flow dynamics in the tubular HCF were analysed using the following 1-D pressure-driven gas flow equation which is based on a circularly shaped core [7]:

$$\frac{\partial P}{\partial t} = \frac{r^2}{8\mu} \frac{\partial}{\partial x} \left(P \frac{\partial P}{\partial x} \right) \quad (1)$$

where P , μ , t and x are the pressure, the dynamic viscosity, the time and the position, respectively. Using Eq. (1) and considering our measurement conditions, the boundary condition was set to one atmospheric pressure because the filling source was the atmospheric air surrounding the HCF. The initial internal gas pressure inside the fibre was set to be 0 Pa; this would not be exact in reality but has been shown to provide a good fit to previous experimental data on pressure driven gas flow into as-drawn HCFs [5]. The diameter of the core was measured from the SEM as $2r_{core} = 18.6 \mu\text{m}$ as well as the average hole diameter of the outer cladding tubes, $2r_{outer} = 9.29 \mu\text{m}$. The fibre length $L = 36.75 \text{ m}$ and $\mu_{air} = 1.82 \times 10^{-5} \text{ kg}/(\text{m}\cdot\text{s})$ [8]. The spatial distributions of the gas in the core and the outer tubes were calculated using Eq. (1) with the parameters described above for three different times (Fig. 2(d)) and, by integrating the pressure distribution along the fibre length, Eq. (1) gives the average pressure inside a tube. In Fig. 2(e), the average pressure inside the core and the outer tube are compared; since the core is larger than the outer tube, the gas filling speed in the core is faster than in the outer tube. Here, our interest is the time dynamics of the pressure contrast between the core and the outer tubes, i.e. the pressure difference ($\Delta P = P_{core} - P_{outer}$); this was calculated and is also shown in Fig. 2(e). ΔP reaches a maximum at 1.87 hours while the gas filling process into the core and the outer tubes is in progress, and gradually decreases until ~15 hours at which the pressure in the outer tubes reaches equilibrium. In Fig. 2(f) this calculated ΔP is compared with the change in the normalised transmitted power (ΔI) from the experimental results, there is clearly a strong agreement between the experiment and the gas flow simulations in terms of the peak position and the decay time. This indicates that the transient differential pressure between the core and the outer tubes leads to the changes in loss in the as-drawn HCF when it is opened up to atmospheric pressure.

The experimental results and the comparison with the gas flow model are clear indications that the pressure contrast between the core and the outer tubes produced the GDRI effect. These results support that the GDRI effect occurs for as-drawn fibres and temporarily changes the optical properties, including confinement loss and bend loss [4] until the pressures inside the core and the outer tubes reach equilibrium with the surrounding atmosphere. The exact relation between differential pressure and change in fibre transmission loss can be analysed numerically e.g. in COMSOL Multiphysics® [4], although Fig. 2(f) indicates a relatively linear relationship for our fibre parameters. For NANFs, the dynamics of the pressure contrast is more complicated to analyse because of the secondary inner tube inside the outer tube which creates an additional crescent-shaped gas channel.

3. DISCUSSION AND CONCLUSION

The findings in this paper are important for accurate characterisation of a HCF. The cut-back method is a standard loss measurement technique whereby transmission of a long length of fibre is measured before the fibre is cut back to a shorter length, at which point the transmission is measured again. Throughout the measurement the optical launch condition remains consistent. The difference between the fibre transmission measurements along with knowledge of the length of the fibre cut off enables the estimation of the fibre loss. When characterising a freshly drawn HCF, the subsequent air flow during the cut-back measurement would produce non-uniform loss along the fibre length and could lead to an inaccurate loss measurement, as while the internal gas pressure is still equalising this loss profile along the fibre will still be evolving. Subsequently, measurement inaccuracies could be created if after loss characterisation the HCF is then stored with sealed ends while the average pressure inside the fibre is still sub-atmospheric. In this case subsequent opening and sealing as-drawn HCF's ends (e.g. repeated splicing) could lead to changes in throughput power due to equalising gas pressures during each measurement.

Considering that the gas flow dynamics are related to the loss change in the as-drawn fibre, this indicates that the fibre structure (core and cladding hole sizes and shapes) and the fibre length could be important parameters (gas filling time, $t_{fill} \propto (L/2r)^2$ [6]). In addition, the wavelength dependence of the changes in loss due to GDRI need to be carefully

considered [4]. Further investigation is underway using COMSOL loss simulations to evaluate the dependence of fibre structure, fibre length and wavelength in more detail.

In conclusion, the impact of the sub-atmospheric as-drawn pressure in a HCF combined with the GDRI effect on transmitted power was demonstrated using NANF and tubular HCF. Gas flow modelling supports the understanding that transient differential pressure between the fibre core and the outer cladding elements was produced due to the different air filling rates because of their different hole sizes. This temporarily decreases the loss of as-drawn HCFs by the GDRI effect. Careful consideration of this transient loss improvement could be necessary to accurately measure the optical properties of a HCF post-fabrication.

This project gratefully acknowledges funding from the Royal Society (University Research Fellowship, N.V. Wheeler), EPSRC Programme grant Airguide Photonics (EP/P030181/1) and the EPSRC Future Photonics Hub (EP/N00762X/1).

References

- [1] A. Nespola, S. R. Sandoghchi, L. Hooper, M. Alonso, T. D. Bradley, H. Sakr, G. T. Jasion, E. N. Fokoua, S. Straullu, F. Garrisi, G. Bosco, A. Carena, A. M. R. Brusin, Y. Chen, J. R. Hayes, F. Forghieri, D. J. Richardson, F. Poletti and P. Poggiolini, "Ultra-long-haul WDM transmission in a reduced intermodal interference NANF hollow-core fiber," in *Proc. Optical Fiber Communications Conference and Exhibition*, 2021, F3B.5 1-3.
- [2] X. Zhu, D. Wu, Y. Wang, F. Yu, Q. Li, Y. Qi, J. Knight, S. Chen and L. Hu, "Delivery of CW laser power up to 300 watts at 1080 nm by an uncooled low-loss anti-resonant hollow-core fiber," *Opt. Express*, vol. 29, no. 2, pp. 1492-1501, 2021.
- [3] W. S. M. Brooks, M. Partridge, I. A. Davidson, C. Warren, G. Rushton, J. Large, M. Wharton, J. Storey, N. V. Wheeler and M. J. Foster, "Development of a gas-phase Raman instrument using a hollow core anti-resonant tubular fibre," *Journal of Raman Spectroscopy*, vol. 52, no. 10, pp. 1-11, 2021.
- [4] T. W. Kelly, P. Horak, I. A. Davidson, M. Partridge, G. T. Jasion, S. Rikimi, A. Taranta, D. J. Richardson, F. Poletti, and N. V. Wheeler, "Gas-induced differential refractive index enhanced guidance in hollow-core optical fibers," *Optica*, vol. 8, no. 6, pp. 916-920, 2021.
- [5] S. Rikimi, Y. Chen, M. T. Partridge, I. A. Davidson, G. T. Jasion, T. D. Bradely, A. A. Taranta, F. Polleti, M. N. Petrovich, D. J. Richardson, and N. V. Wheeler, "Pressure in As-drawn Hollow Core Fibers," in *Proc. OSA Advanced Photonics Congress*, 2020, SoWIH.4 1-2.
- [6] R. Wynne and B. Barabadi, "Gas-filling dynamics of a hollow core photonic bandgap fiber for nonvacuum conditions," *Appl. Opt.*, vol. 54, no. 7, pp. 1751-1757, 2015.
- [7] J. Henningsen and J. Hald, "Dynamics of gas flow in hollow core photonic bandgap fibers," *Appl. Opt.*, vol. 47, no. 15, pp. 2790-2797, 2008.
- [8] J. A. Bearden, "A Precision Determination of the Viscosity of Air," *Phys. Rev.*, vol. 56, no. 10, pp. 1023-1040, 1939.